Electronic Supplementary Material (ESI) for Physical Chemistry Chemical Physics.

Supplementary Information for

One-step Functionalization of Mildly and Strongly Reduced Graphene Oxide with Maleimide: An Experimental and Theoretical Investigation of the Diels-Alder [4+2] Cycloaddition Reaction

Alfonso Ferretti,[1] Sourab Sinha,[2] Luca Sagresti,[2,3] Esteban Araya-Hermosilla,[4] Mirko Prato,[5] Virgilio Mattoli,[4] Andrea Pucci,[5,6] and Giuseppe Brancato[2,3*]

1. *Università di Pisa, Dipartimento di Ingegneria Civile ed Industriale, Largo Lucio Lazzarino 2, I-56124 Pisa, Italy.*
2. *Scuola Normale Superiore, Piazza dei Cavalieri 7, I-56126 Pisa, Italy and CSGI.*
3. *Istituto Nazionale di Fisica Nucleare (INFN) sezione di Pisa, Largo Bruno Pontecorvo 3, 56127 Pisa, Italy.*
4. *Center for Materials Interfaces, Istituto Italiano di Tecnologia Viale Rinaldo Piaggio 34, 56025 Pontedera, Italy.*
5. *Materials Characterization Facility, Istituto Italiano di Tecnologia, Via Morego 30, 16163 Genoa, Italy.*
6. *Department of Chemistry and Industrial Chemistry, University of Pisa, Via Moruzzi 13, 56124 Pisa, Italy.*
7. *CISUP, Centro per l'Integrazione della Strumentazione dell'Università di Pisa, Lungarno Pacinotti 43, 56126 Pisa, Italy.*

Corresponding authors:

E-mail: giuseppe.brancato@sns.it

Content

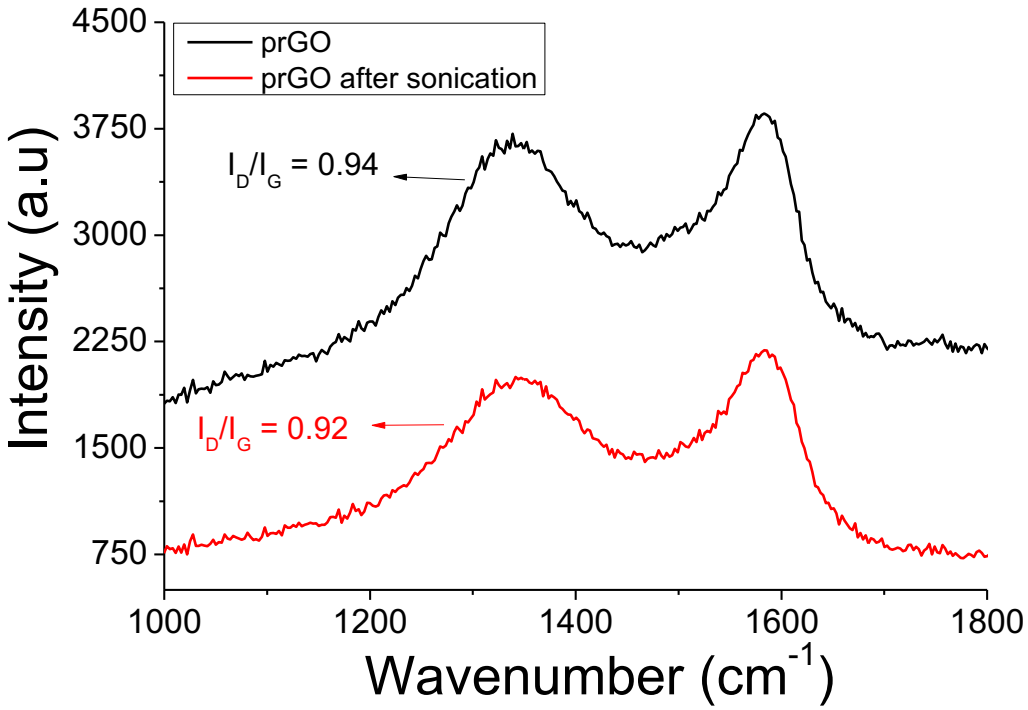

Figure 1 Raman spectra of prGO before and after sonication.

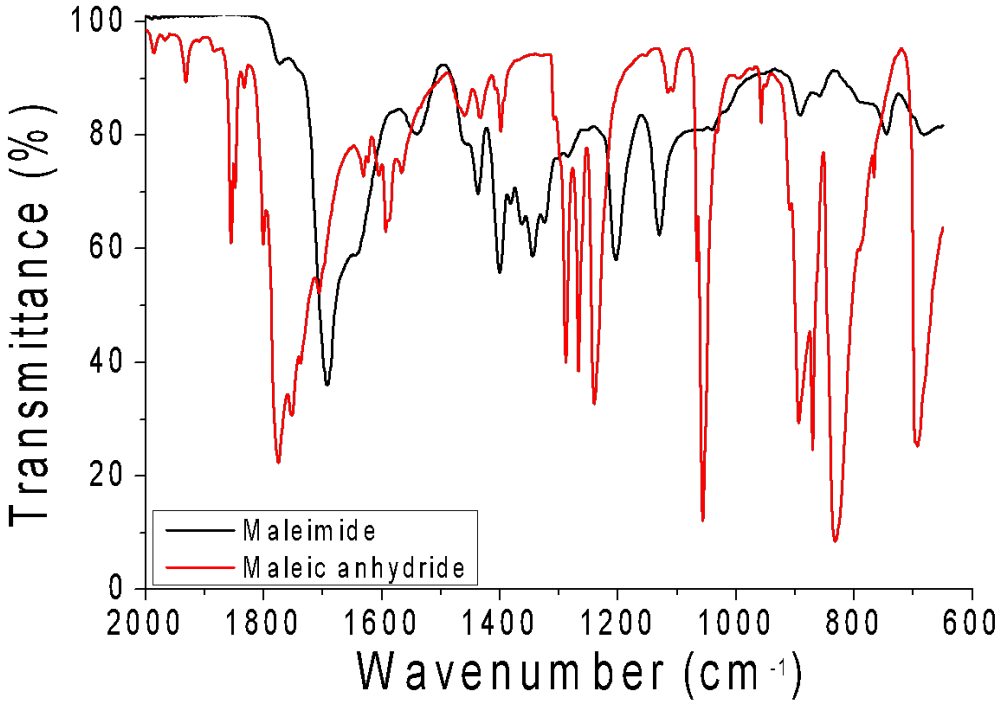

Figure 2 ATR-FT-IR spectra of the maleimide derivative (black line) and maleic anhydride (red line).

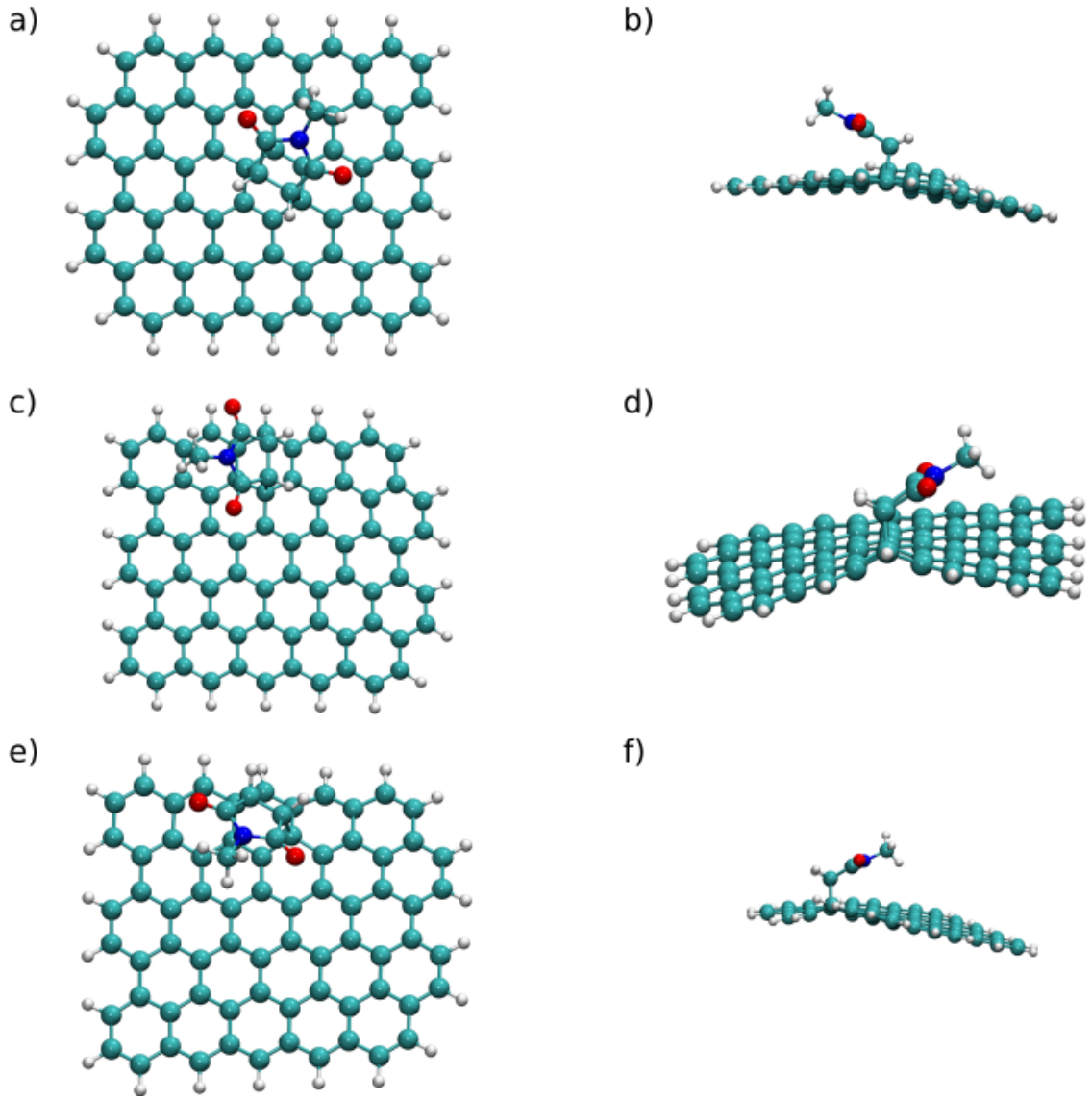

Figure 3 Top and side view of the model (a, b) 1aP, (c, d) 1bP, and (e, f) 1cP.

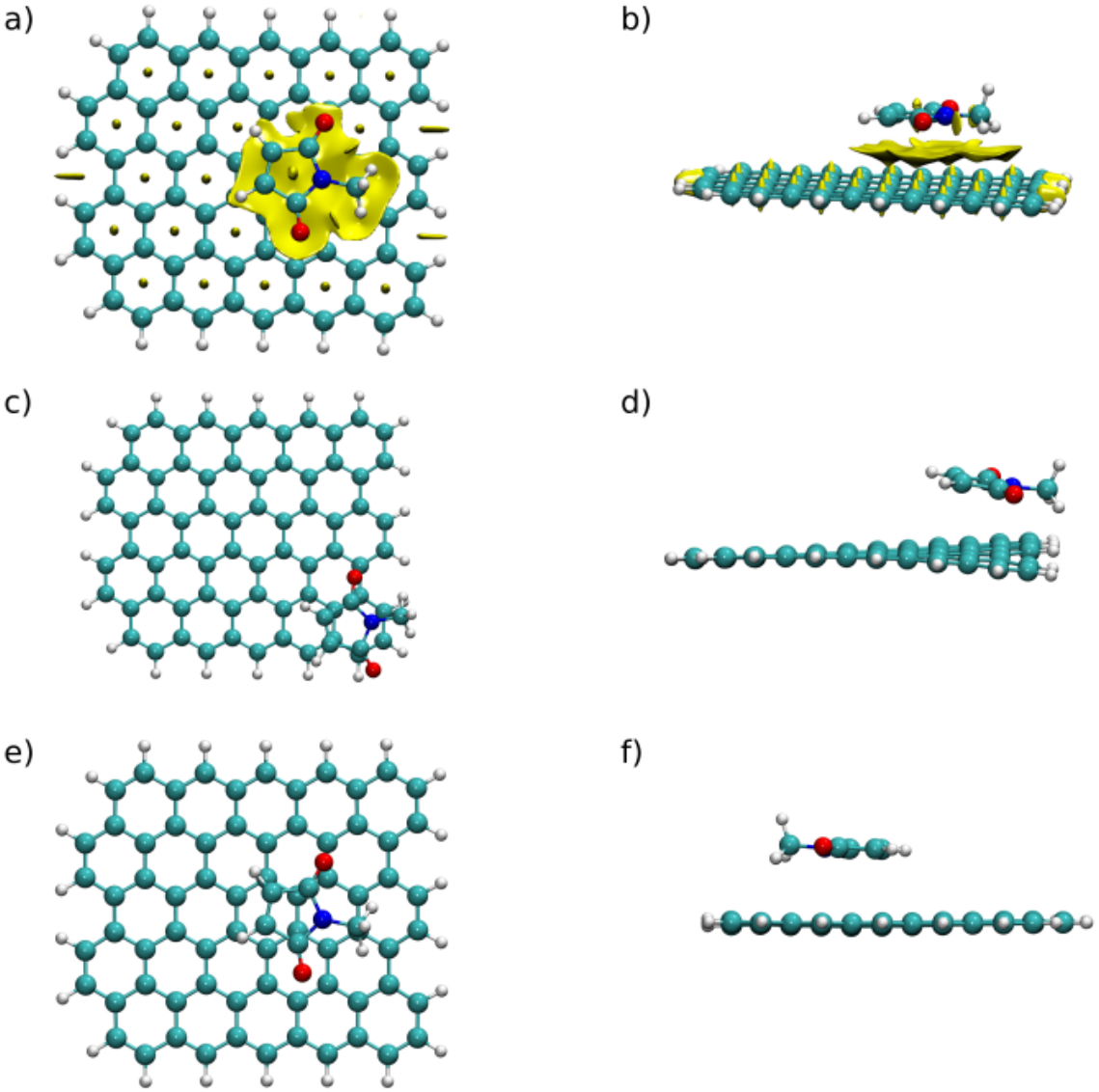

Figure 4 Top and side views of the non-covalent interaction surface for the model (a, b) 1eP, (c, d) 1dP, and (e, f) 1eP. In a) and b), the non-covalent interaction isosurface is depicted as obtained using the MultiWFN software.

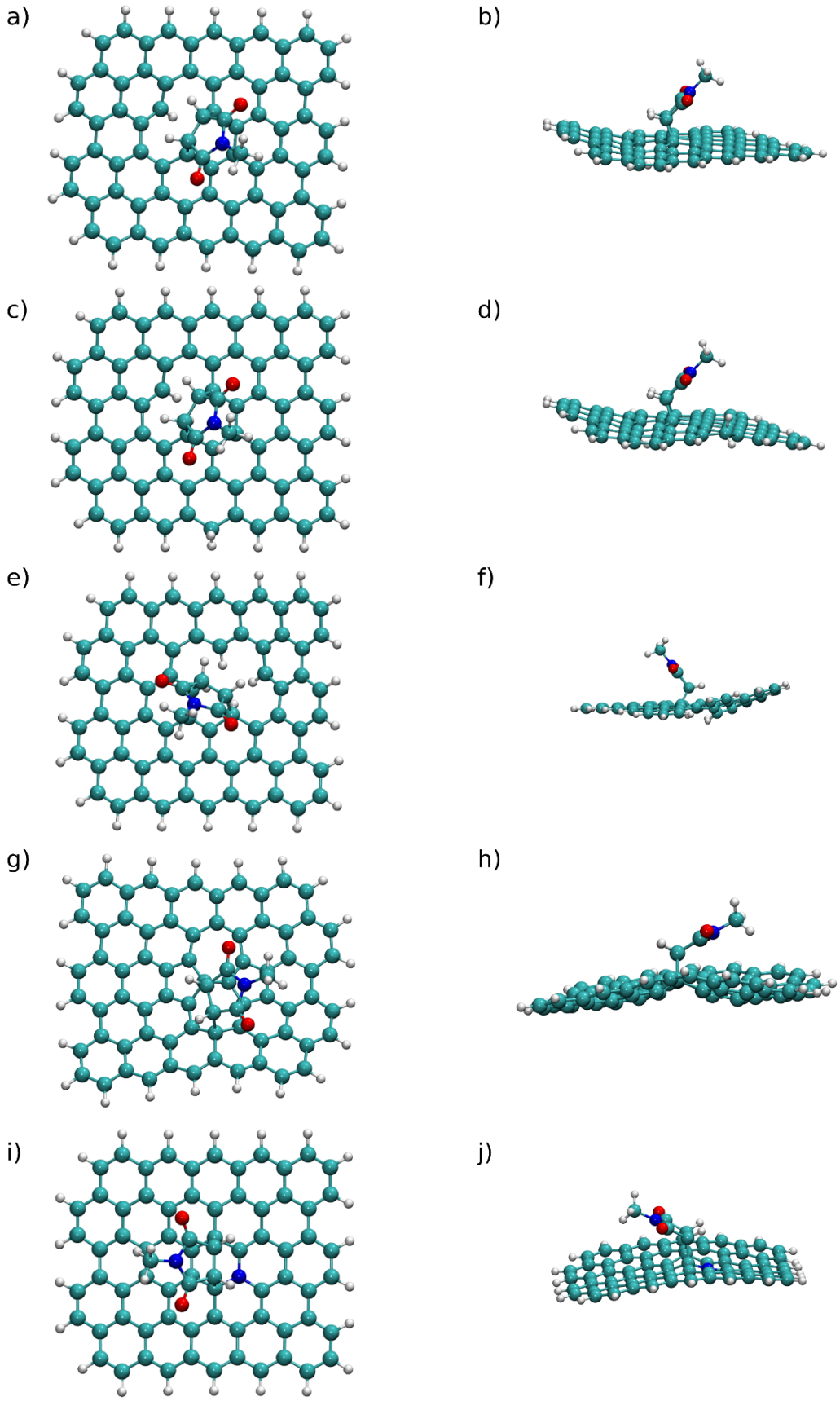

Figure 5 Top and side views of the model (a, b) 2P, (c, d) 3P, (e, f) 4P, (g, h) 5P, and (i, j) 6P.

Table 1: Geometrical parameters of the optimized geometry of the maleimide-graphene adducts. The definition of the geometrical parameters is reported in Figure 5. Angles are in degree, bonds in Å.

Graphene Product Model	Dihedral Angle	Maleimide Tilting Angle	Maleimide C=C Bond Length	Maleimide-Graphene Bond Length
1Pa Central	28.2	25.9	1.53	1.65
1Pb External	30.5	26.9	1.54	1.58
1Pc Internal	29	26	1.53	1.63
1Pd Non-Covalent Border			1.33	3.2
1Pe Non-Covalent Center			1.33	3.19
2P Vacancy Radical	36.7	53.9	1.53	1.54
3P Vacancy External H	36.8	56.9	1.53	1.54
4P Double Vacancy (585 divacancy)	37.8	55	1.53	1.56
5P Stone Wales Defect	28.1	33	1.57	1.6
6P Nitrogen Doped	31.6	28.2	1.54	1.6
7P Double Epoxy Central	30.1	28	1.56	1.59
8P Double Epoxy External	31.5	31.2	1.55	1.58
9P Tetra-Epoxy	33.7	25.3	1.56	1.58
10P Double Hydroxyl Epoxy	30.8	26.7	1.57	1.58

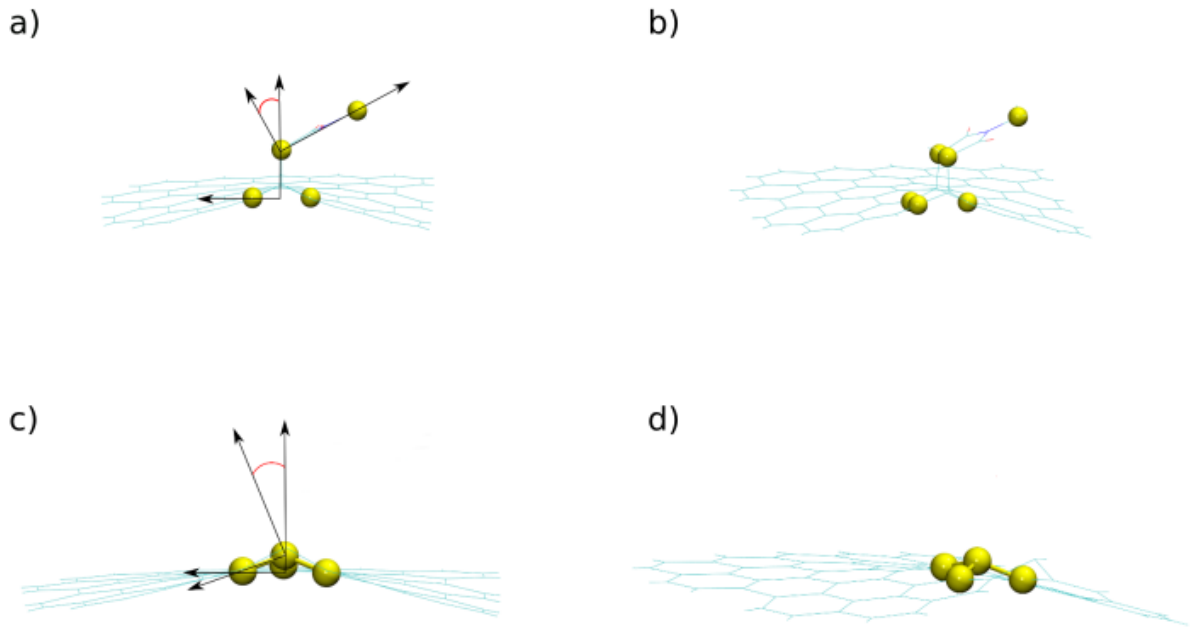

Figure 6 (a, b) Tilting angle between maleimide molecular axis (i.e., the vector connecting the C=C middle point to the carbon atom belonging to the methyl group) and local graphene plane (i.e., three adjacent carbon atoms are used to identify the local plane). Note that it was considered the complementary angle between maleimide molecular axis and the normal to the local graphene plane. (c, d) Orthogonal and rotated view of the four carbon atom coordinates used to evaluate the local graphene dihedral angle (i.e., improper dihedral), represented in red.

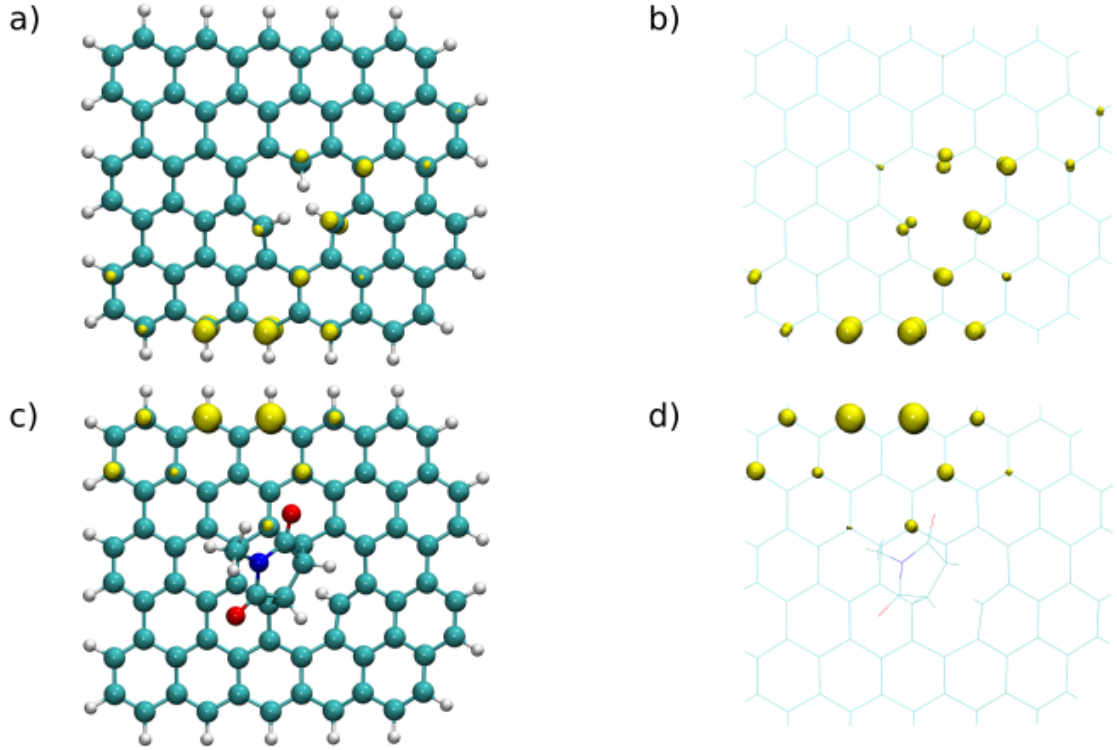

Figure 7 Spin density isosurface of the (a,b) 2R and (c,d) 2P vacancy radical systems.

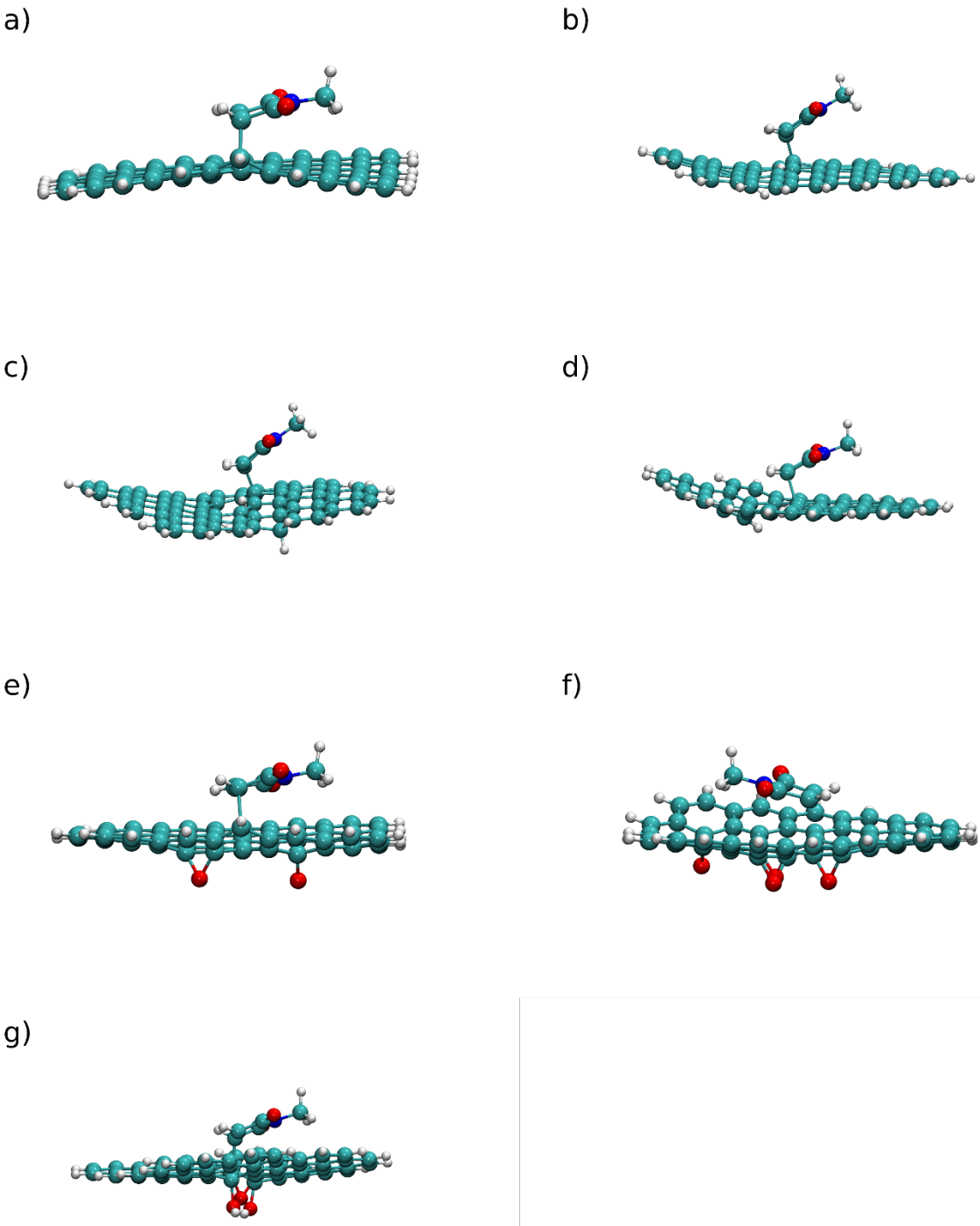

Figure 8 Side view of the model (a) 1bTS, (b) 2TS, (c) 3TS, (d) 4TS, (e) 8TS, (f) 9TS, and (g) 10TS.

Table 2: Solvent (i.e., chloroform and acetonitrile) and temperature effects on the reaction enthalpy (ΔH) of all systems. Thermal effects are evaluated as the difference ΔE(T=323.15K) - ΔE(T=0K) (including zero-point energy). Chloroform and acetonitrile effects are evaluated as the difference ΔE(T=0K, solvent) - ΔE(T=0K, gas-phase).

Model	Thermal corr. (323.15K)	Solvent effects (chloroform)	Solvent effects (acetonitrile)
1a Central	-0.7	5.0	
1b External Border	-0.6	1.0	1.1
1c Internal Border	-0.5	3.0	
1d Non-Covalent Border	-0.7	1.2	
1e Non-Covalent Center	0.6	1.3	1.2
2 Vacancy Radical	-0.6	0.1	
3 Vacancy Hext	-1.0	1.4	2.3
4 Double Vacancy	-0.4	-0.1	
5 Stone Wales	-0.9	-1.2	
6 Nitrogen Doped	-1.1	2.7	
7a Double Epoxy Central	-1.1	1.0	6.0
8 Double Epoxy External	-0.9	0.7	
9 Tetra Epoxy	-1.0	0.9	1.4
10 Double Hydroxyl Epoxy	-0.9	0.8	

Table 3: Reaction enthalpy and Gibbs free energy (in kcal/mol) for all relevant models.

Reaction	Activation enthalpy		Binding enthalpy		Activation free energy		Binding free energy	
	Gas	**Solvent**	**Gas**	**Solvent**	**Gas**	**Solvent**	**Gas**	**Solvent**
1R → 1Pb	5.4	4.8	-12.2	-11.4	21.6	23.8	3.4	7.3
1R → 1Pe			-16	-14.6			-3.4	-0.1
2R → 2P	27.3	27.5	-8	-8	41.8	43.2	6.3	8.8
3R → 3P	21.3	21.7	-29.3	-28.1	36.7	38.1	-13.4	-10.4
4R → 4P	16.6	17	-9.1	-9.2	31.5	33	5.7	7
7R → 7Pa			-37.9	-36.9	13.4	15.6	-20.5	-18.4
8R → 8P	4.1		-15.5	-15	19	16.4	0	2.6
9R → 9P	3.6	4.9	-36.1	-35.3	19.3	21.9	-19.3	-16.7
10R → 10P	3.5	3.9	-28.9	-28.1	19.1	21.6	-12.7	-9.8

Table 4: Geometrical parameters of the optimized transition states of the maleimide-graphene adducts. Angles are in degree, bonds in Å.

Transition State Model	Dihedral Angle	Maleimide Tilting Angle	Maleimide C=C Bond Length	Maleimide-Graphene Bond Length
1bTS External	9.5	18.8	1.47	1.66-2.54
2TS Vacancy Radical	10.1	44.9	1.5	1.6-2.27
3TS Vacancy External H	6.3	42.1	1.48	1.64-2.38
4TS Double Vacancy	17.7	32.5	1.42	2.01-2.07
8TS Double Epoxy External	1.6	22.8	1.41	1.96-2.85
9TS Tetra-Epoxy	11.7	21.2	1.4	2.23-2.37
10TS Double Hydroxyl Epoxy	9.6	28.5	1.49	1.63-2.57

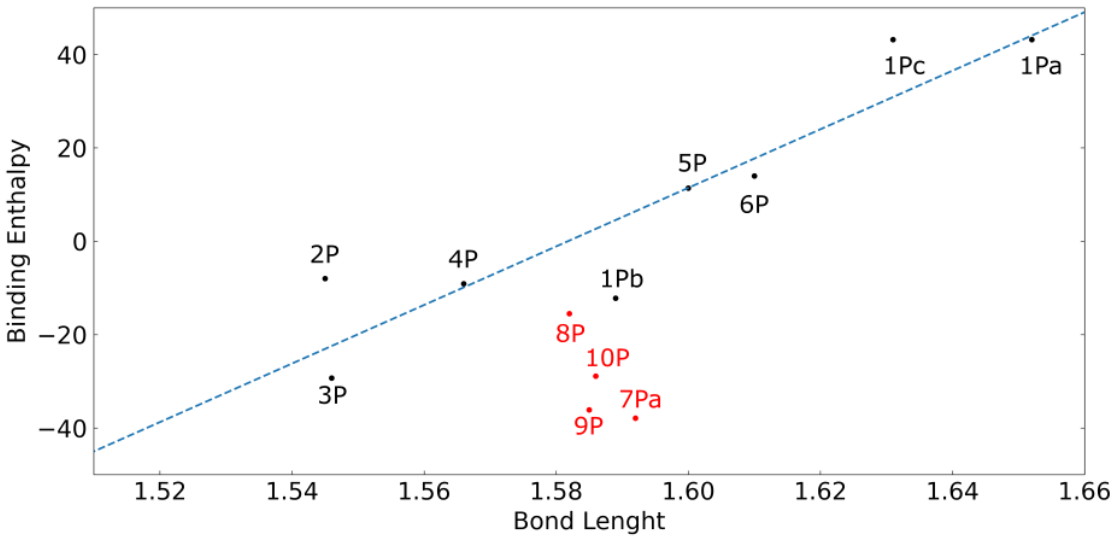

Figure 9: Correlation between maleimide-graphene bond length (Table 1) and binding enthalpy. Products obtained from defect-free and defective graphene models (black dots) show a good degree of correlation (linear fitting represented as a dashed line). On the contrary, oxygen-functionalized adduct models (red dots) do not show any apparent correlation.

a)

1R Pristine Graphene	Local Nucleophilicity	Local Electrophilicity
C1	2.31	-1.52
C2	-2.22	-2.28
C3	-0.68	-0.63
C4	-0.68	-0.63
C5	-2.22	-2.28
C6	-1.47	-1.52
C7	-1.96	-1.88
C8	-1.23	-1.15
C9	-0.44	-0.31
C10	-1.30	-1.06
C11	-13.08	-14.03
C12	-1.65	-1.57

b)

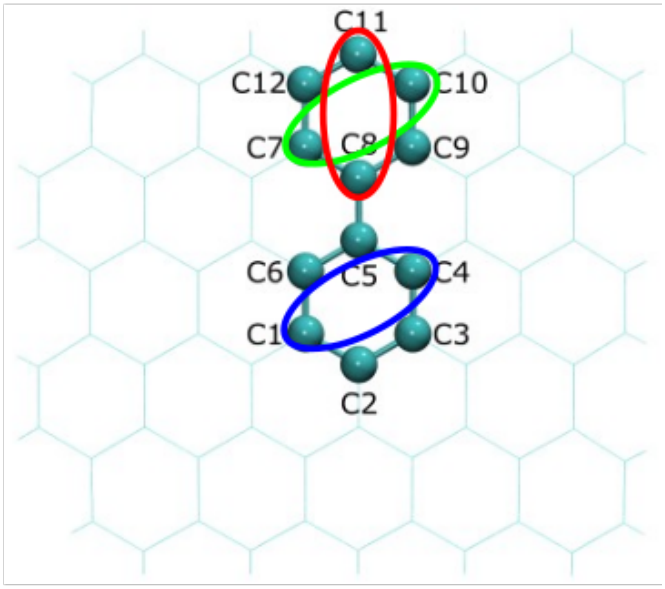

c)

2R Vacancy Radical	Local Nucleophilicity	Local Electrophilicity
C1	-4.24	-4.18
C2	-1.25	-1.52
C3	-1.42	-1.25
C4	0.00	0.01
C5	-0.74	-0.55
C6	-0.27	-0.19
C7	-2.10	-2.31
C8	-0.74	-0.37
C9	-5.92	-6.56
C10	-0.61	-1.11
C11	-4.68	-4.61
C12	-0.66	-0.62

d)

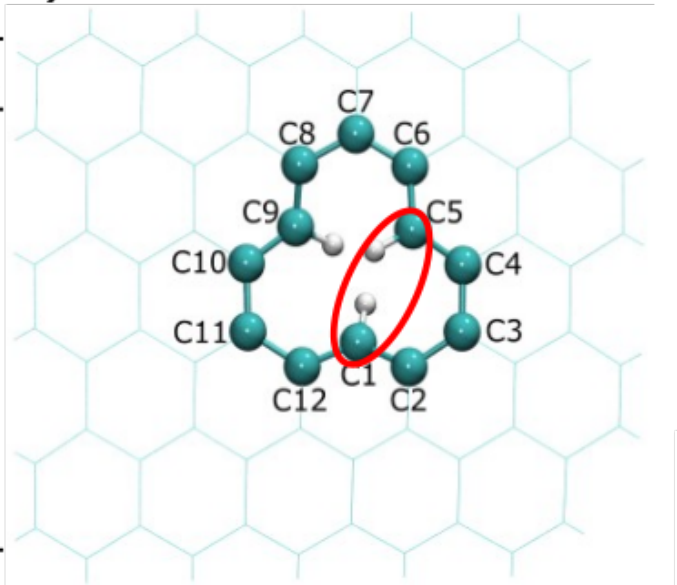

Figure 10 Fukui Analysis reported with images showing the selected atoms for models (a, b) 1R and (c, d) 2R.

a)

3R Vacancy External H	Local Nucleophilicity	Local Electrophilicity
C1	-14.48	-9.25
C2	-1.09	-0.59
C3	-0.83	-1.39
C4	0.18	-1.16
C5	7.77	-10.63
C6	0.26	-0.06
C7	6.77	-19.51
C8	-0.73	-1.33
C9	-14.86	-22.11
C10	0.10	-1.56
C11	-17.17	-11.86
C12	0.10	-0.59

b)

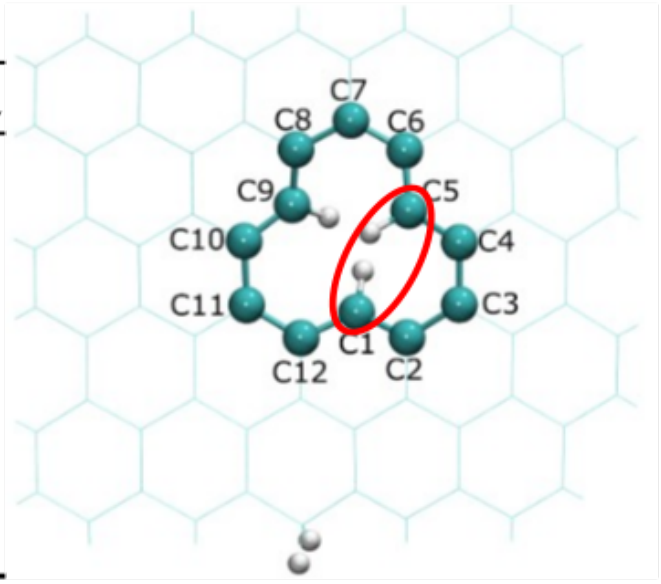

c)

4R Double Vacancy	Local Nucleophilicity	Local Electrophilicity
C1	-0,56	-3,59
C2	-0,27	-0,05
C3	-2,35	-6,06
C4	-0,50	-3,17
C5	-1,85	-6,16
C6	-2,26	-0,27
C7	-11,69	0,16
C8	-1,50	-1,32
C9	-0,81	-2,00
C10	-1,32	-0,85
C11	-2,50	-0,10
C12	-4,05	-1,08
C13	-0,98	0,08
C14	-0,35	-1,92

d)

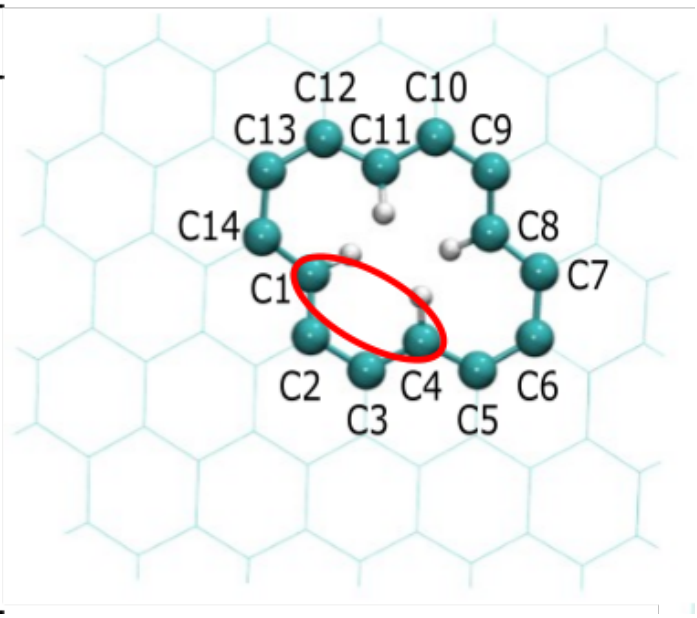

Figure 11 Fukui Analysis reported with images showing the selected atoms for models (a, b) 3R and (c, d) 4R.

a)

5R Stone Wales Defect	Local Nucleophilicity	Local Electrophilicity
C1	-3,13	-4,74
C2	-0,95	-1,01
C3	-0,72	-0,42
C4	-3,43	-2,13
C5	-3,43	-2,13
C6	-0,72	-0,42
C7	-7,12	-1,83
C8	-0,34	-0,28
C9	-3,53	-4,71
C10	-0,85	-1,20

b)

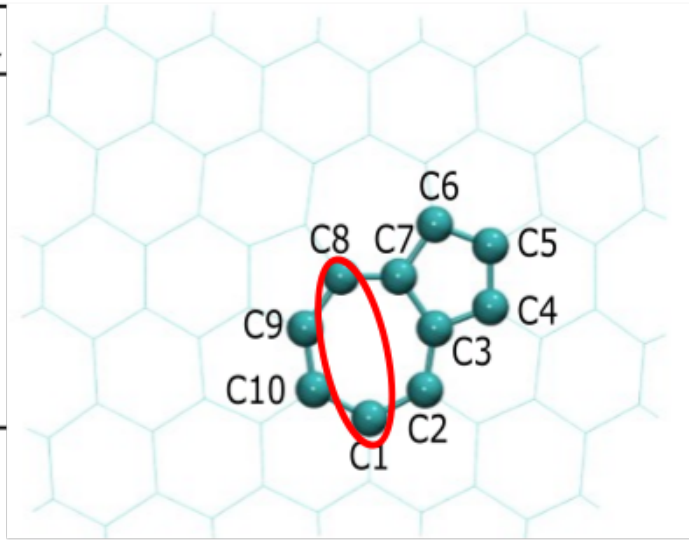

c)

6R Nitrogen Substitutional	Local Nucleophilicity	Local Electrophilicity
N1	-4,22	-0,80
C2	-1,86	-2,42
C3	-0,39	-0,32
C4	-0,65	-0,52
C5	-2,68	-0,30
C6	-0,42	0,05
C7	-2,29	-0,14
C8	0,12	-1,12
C9	-0,85	-0,16
C10	-0,98	-2,40
C11	-1,36	-0,53
C12	-6,28	-0,05
C13	-1,16	-0,65

d)

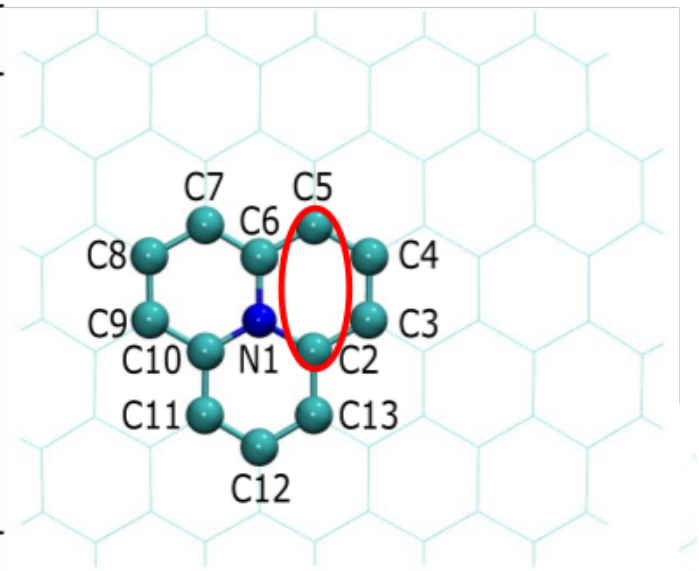

Figure 12 Fukui Analysis reported with images showing the selected atoms for models (a, b) 5R and (c, d) 6R.

a)

7R Double Epoxy	Local Nucleophilicity	Local Electrophilicity
C1	-7.87	-5.52
C2	-0.52	-0.49
C3	-3.06	-2.51
C4	-0.44	-0.51
C5	-8.42	-6.27
C6	-1.18	-0.66
C7	-0.20	-0.39
C8	-1.72	-1.97
C9	-1.21	-0.65
C10	-0.72	-0.52
C11	0.46	-0.05
C12	0.34	0.24
C13	-2.53	-2.11

b)

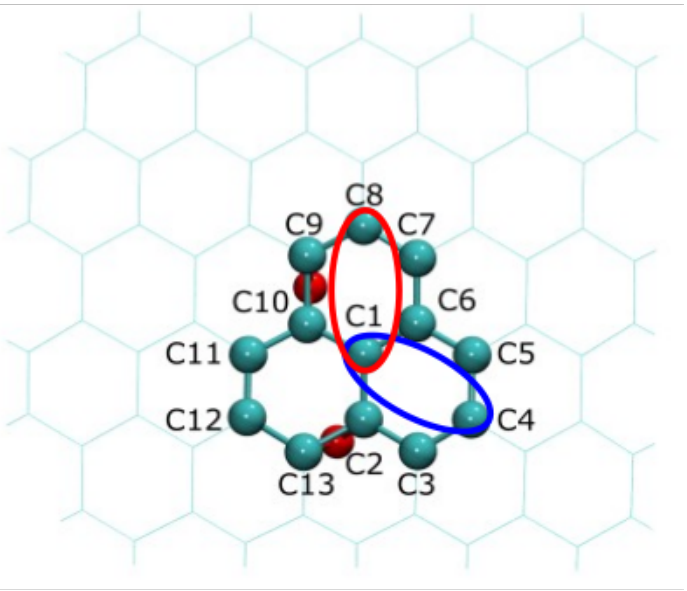

c)

8R Double Epoxy External	Local Nucleophilicity	Local Electrophilicity
C1	-0,62	0,09
C2	-0,48	-2,23
C3	-0,73	-1,04
C4	-0,86	0,17
C5	-1,31	-0,33
C6	-0,74	-1,91
C7	-1,98	-2,70
C8	-0,76	-2,12
C9	-0,78	-0,03
C10	-0,82	-0,29
C11	-1,29	-0,72
C12	-14,95	-7,27
C13	-1,16	-0,61

d)

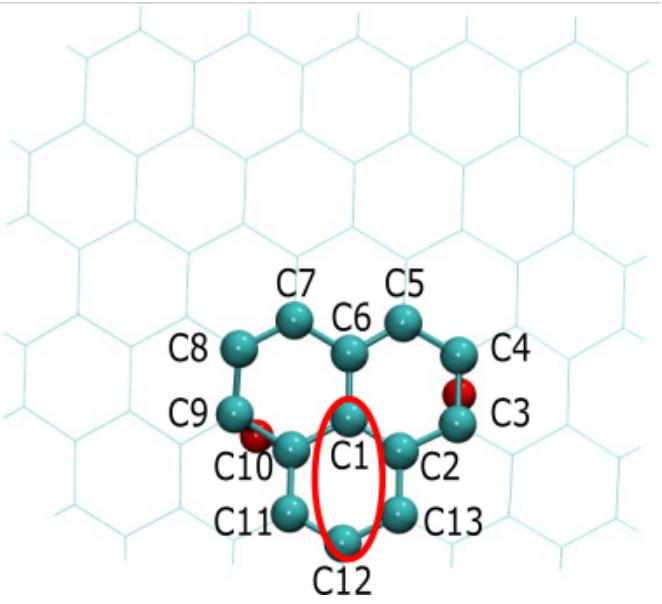

Figure 13 Fukui Analysis reported with images showing the selected atoms for models (a, b) 7R and (c, d) 8R.

a)

9R Tetra epoxy	Local Nucleophilicity	Local Electrophilicity
C1	-0,13	-0,15
C2	-1,51	-1,62
C3	-0,32	-0,46
C4	-0,56	-0,22
C5	-1,65	-1,05
C6	-0,12	-0,02
C7	-0,39	-0,36
C8	-0,23	-0,51
C9	-0,41	-0,20
C10	-0,44	-0,38
C11	-0,45	-0,64
C12	-0,64	-0,75
C13	-0,36	-0,36
C14	-0,03	0,13
C15	-0,49	-0,32
C16	-1,44	-2,06

b)

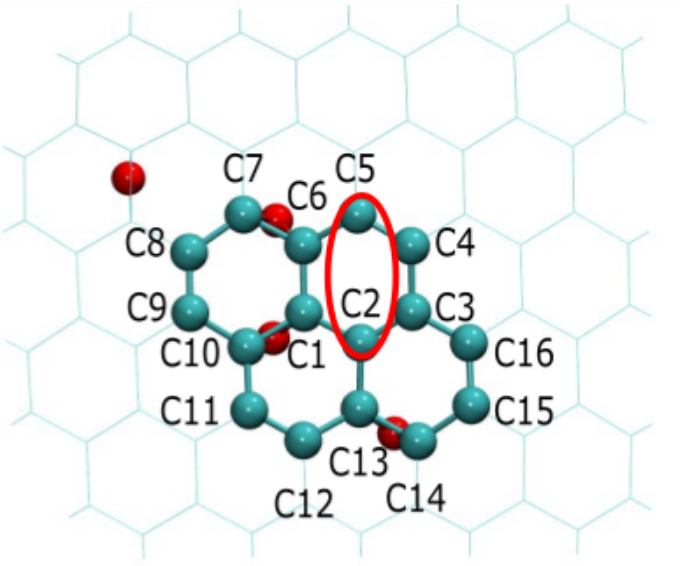

c)

10R Double Hydroxy Epoxy	Local Nucleophilicity	Local Electrophilicity
C1	-5,65	-2,12
C2	-2,50	-5,12
C3	-2,07	-1,60
C4	-142,12	-6,59
C5	-2,03	-3,42
C6	-1,20	-4,19
C7	-4,67	-2,93
C8	0,15	0,18
C9	-1,46	-0,94
C10	-0,80	-0,49
C11	-1,90	-0,99
C12	0,52	-0,17
C13	-1,27	0,20

d)

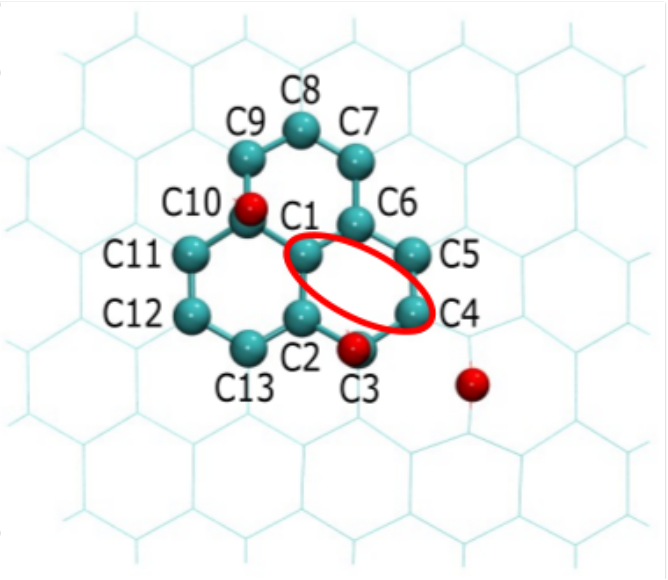

Figure 14 Fukui Analysis reported with images showing the selected atoms for models (a, b) 9R and (c, d) 10R.